

CuMnS@rGO Nanocomposite as Electrode Material for Photovoltaic Applications

F. Michael Raj^{*1}, A. Jakob Anbarasu¹, A. Anitha¹ and Soven Dhawa²

¹ Post Graduate Department of Chemistry, Arul Anandar College, Karumathur, Madurai - 625 514, Tamil Nadu, India

² Department of Chemistry, Dr. MGR Educational and Research Institute, Chennai - 600 095, Tamil Nadu, India

Abstract

Transition metal sulfides nanocomposites have indeed garnered significant interest in the field of energy storage devices due to their unique features. These materials offer several advantages that make them promising candidates for applications such as batteries, solar cells, super capacitors etc. Twisted leaves like CuMnS@rGO nanocomposites were synthesized by co-precipitation method using sodium sulfide, Copper acetate and Manganese acetate as the precursors. X-ray diffraction studies (XRD) revealed that the synthesized CuMnS@rGO nanostructures were hexagonal structure with particle size 2.5 nm which is calculated from the XRD pattern using Debye Scherer's method. The bandgap value was computed from the UV-Vis spectrum by Tauc's plot as 2.2 eV. The electrochemical properties were examined by dielectric studies and J-V Characteristic studies. This indicates that the CuMnS@rGO electrode possesses high electrocatalytic activity for the reduction of triiodide to iodide at the counter electrode which is due to twisted-leaves-like structure and high specific surface area. As charge transfer resistance (R_{CT}) reduces, photo catalytic activity rises, increasing the solar cells overall efficiency (DSSCs).

Key words: Electro catalytic activity, Reduced graphene oxide, Solar cell, Dielectric studies, CuMnS@rGO

The dye-sensitized solar cell (DSSC) technology, pioneered by O'Regan and Gratzel [1] has garnered substantial interest in both scientific research and industrial applications over the past few decades. This is primarily due to its advantageous characteristics such as low cost, simple fabrication process, renewability, high photoconversion efficiency, and environmental friendliness [2-5]. Typically, DSSCs consist of several key components such as photoanode, transparent conducting oxide, electrolyte and counter electrode. Platinum has conventionally been used as the material for the counter electrode due to its efficient catalytic properties. However, the high cost and scarcity of platinum pose significant limitations to the widespread commercial production of DSSCs. Researchers and industry stakeholders are actively exploring alternative materials and strategies to address this challenge and enhance the cost-effectiveness and scalability of DSSC technology [6].

Ternary metal sulfides, such as CuMnS, CoMnS, CoNiS, have gained significant interest in the development of low-cost solar cells due to their unique properties and potential applications [7-14]. Among these sulfides, Cupric Manganese sulfide (CuMnS) stands out due to its distinctive characteristics, versatile nature and CuMnS possesses a hexagonal crystal structure. CuMnS unique properties make it suitable for various applications beyond solar cells, including light emitting diodes (LEDs), chemical sensors, lithium-ion batteries, hydrogen evolution, and photocatalysis. In the context of solar cells,

CuMnS@rGO shows promise as an efficient electrocatalytic counter electrode (CE) material due to its excellent activity for I_3^- reduction [15-18].

Research efforts focused on the synthesis, characterization, and optimization of rGO-based nanocomposites are ongoing, aiming to harness its potential for enhancing the performance and cost-effectiveness of solar energy conversion technologies. By further understanding and leveraging the unique properties of CuMnS and other transition metal sulfides, researchers aim to develop next-generation solar cells that are not only efficient but also economically viable and environmentally sustainable.

MATERIALS AND METHODS

Materials

Manganese acetate dihydrate ($(CH_3COO)_3Mn \cdot 2H_2O$), Sodium sulfide flakes ($Na_2S \cdot xH_2O$), Cupric acetate ($Cu(CH_3COO)_2$) and Graphite were purchased from Loba Chemie. The sensitized ruthenium red dye N719 was purchased from Solaronix SA (Switzerland). All reagents were of analytical grade and used without further purification. FTO glass substrates ($12 \Omega \text{ cm}^2$, Solaronix) were cut into $2.5 \times 2.5 \text{ cm}^2$ and ultrasonically cleaned sequentially in acetone and distilled water for 10 mins each and then washed with isopropyl alcohol.

***Correspondence to:** F. Michael Raj, E-mail: fmichaelraj@gmail.com

Synthesis of CuMnS@rGO nanocomposites

About 0.05 g of cupric acetate and manganese acetate were dissolved in a 50 mL of de-ionized water separately and stirred for 20 mins using magnetic stirrer. Then the above contents were transferred into a 100 mL sodium sulphide solution and were treated at 80 °C for reaction time as 12 h to form CuMnS nanoparticles. Using Modified Hummer's method, the graphene oxide was synthesized and reduced by using citric acid. Both the rGO and CuMnS were mixed together to form the CuMnS@rGO nanocomposite as black colored powder. The precipitated solution is centrifuged at high RPM level with ethanol and water. The obtained powder was dried at 60 °C for 12 h in a vacuum drying oven. The schematic illustration of coprecipitation synthesis of CuMnS@rGO nanocomposites (NCs) is shown in (Fig 1).

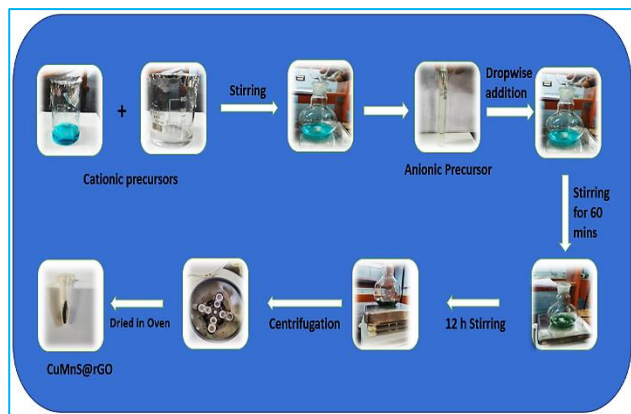


Fig 1 Schematic setup of co-precipitation synthesis of CuMnS@rGO

RESULTS AND DISCUSSION

XRD analysis

XRD patterns as seen in the Fig.2 represents the broad diffraction peaks were observed at 26.5°, 33.15°, 46.5°, 51.7° and 66° correspond to the planes of (002), (101), (103), (110) and (118) representing hexagonal phase [24]. In (Fig 2), the broad peak at 26° and 42° were due to incomplete conversion of Graphene to reduced graphene oxide [25] which were intended narrow peaks in combined with CuMnS nanoparticles.

The predominant peak ($2\theta=26.5$) of plane (002) was found to become sharper with high intensity at 12 h reaction time that confirms the perfect crystalline phase of CuMnS@rGO Nanocomposites. The average crystallite size was calculated by using Scherrer's formula [21] as 2.5 nm.

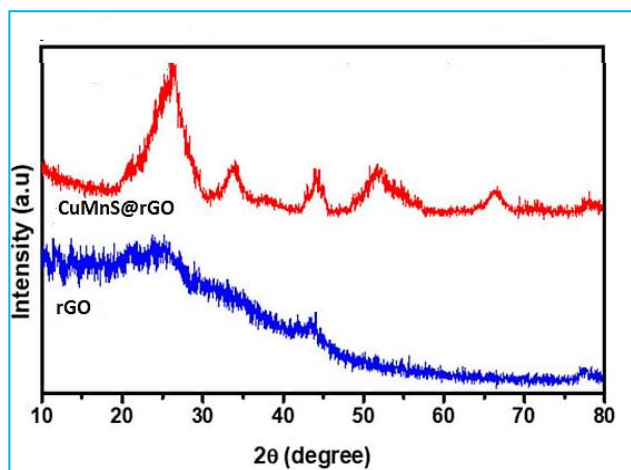


Fig 2 XRD pattern of rGO and CuMnS@rGO nanocomposites

Morphology analysis

The Scanning Electron Microscope (SEM) images of the synthesized CuMnS@rGO nanocomposites, as depicted in (Fig 3a-d), display a distinctive morphology resembling twisted leaves that interlock with one another. This unique structure, characterized by interlaced nano-layers, significantly increases the surface area of the material. The augmented surface area is advantageous for enhancing the electrocatalytic activities of the counter electrode (CE) in dye-sensitized solar cells (DSSCs). Consequently, this morphological feature contributes to the improved photovoltaic performance of DSSCs by facilitating better electron transfer and catalytic processes [27].

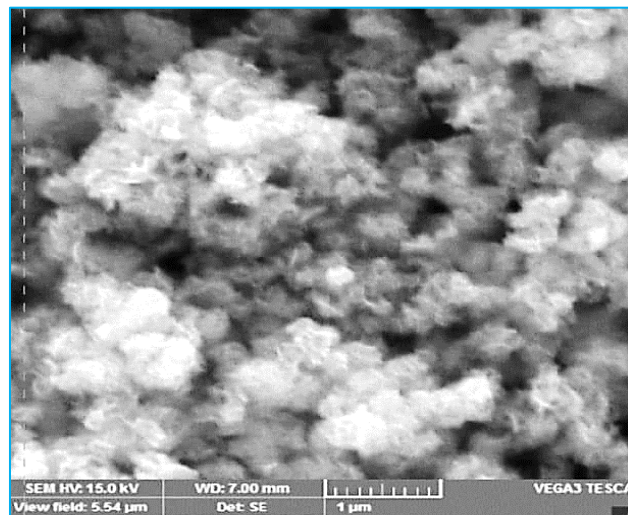


Fig 3 SEM image of CuMnS@rGO nanocomposites

UV-Vis spectroscopic analysis

The absorption spectrum of the synthesized CuMnS@rGO, illustrated in (Fig 4), reveals excitonic peaks at 225 nm and 248 nm. The bandgap energy, determined from the UV-Vis spectrum, is calculated using Tauc's graph method. This involves plotting the square root of the absorption energy (αE , where α is the absorbance and E is the photon energy) against E . From this plot, the bandgap energy is found to be 2.4 eV. This bandgap value is significant for the material's optical properties and its potential applications in optoelectronic devices.

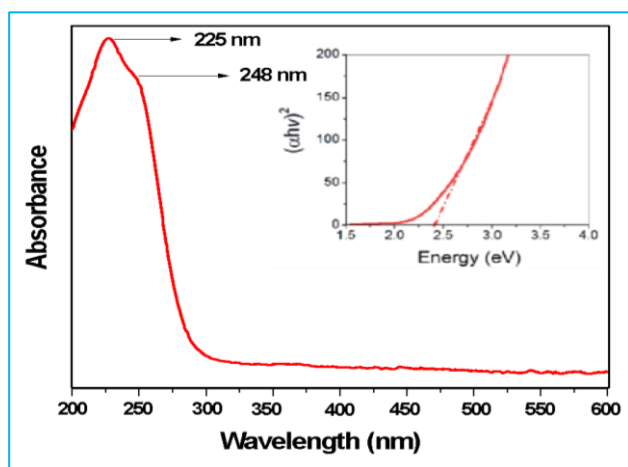


Fig 4 UV-Vis Spectrum of CuMnS@rGO nanocomposites (inside Tauc's plot)

Dielectric studies

Dielectric studies for nanomaterials delve into the exploration and understanding of dielectric properties at the

nanoscale, where the size, shape, and surface characteristics of materials can significantly influence their electrical behavior. These studies are pivotal for the development and optimization

of nanoelectronics devices, energy storage systems, sensors, and other applications where the manipulation of electrical and electromagnetic properties at the nanoscale is crucial.

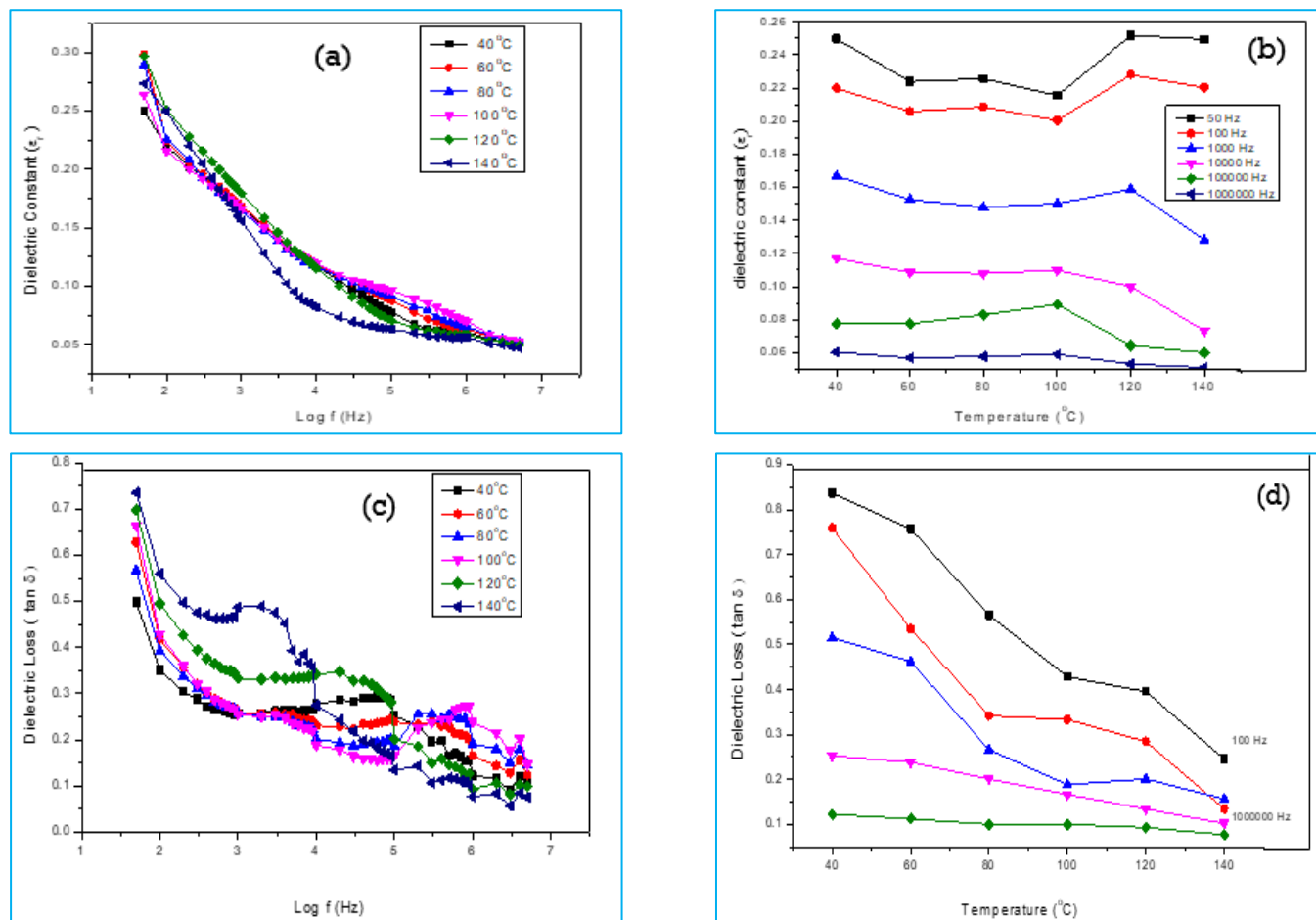


Fig 5 Dielectric studies plot of CuMnS@rGO nanocomposites

(a. Dielectric constant (ϵ_r) vs log frequency at different temperatures, b. Dielectric constant (ϵ_r) vs temperature at different frequencies, c. Dielectric loss vs log frequency at different temperatures, d. Dielectric loss vs temperature at different frequencies)

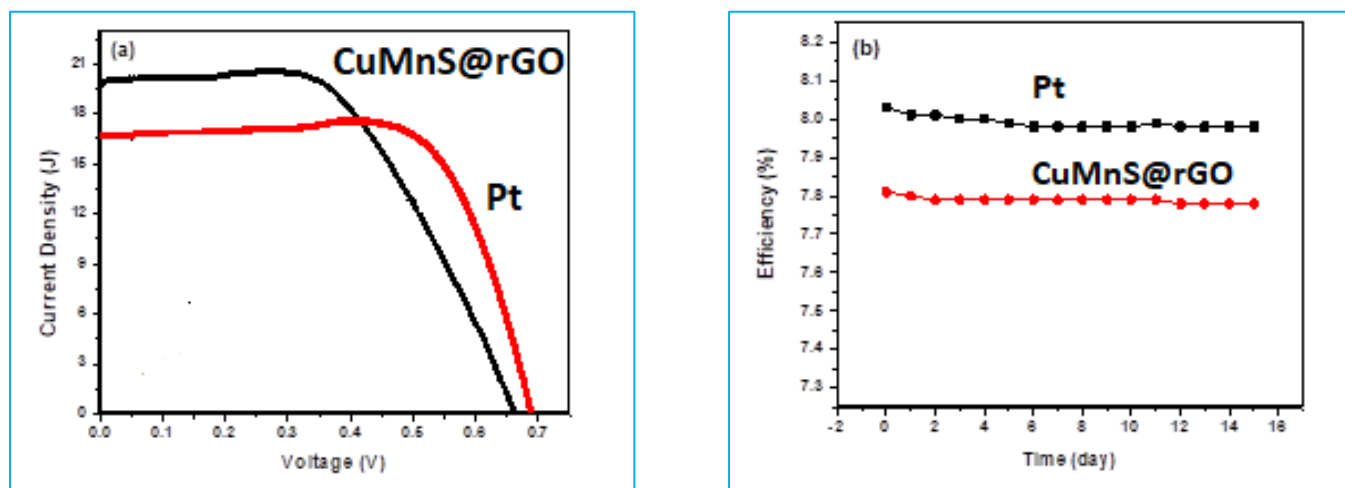


Fig 6 (a) J-V characteristics of DSSCs using Pt and CuMnS@rGO CEs and (b) long term stability of fabricated DSSCs with Pt and CuMnS@rGO CEs

Table 1 Photovoltaic parameters obtained from the J-V curves shown in Fig.6a.

CE	J_{sc} (mA cm ⁻²)	V_{oc} (mV)	FF (%)	η (%)
Pt	16.669	0.689	73.3	8.03
CuMnS@rGO	19.859	0.661	64.2	7.81

J-V characteristics studies

The photocurrent density-voltage (J-V) curves for dye-sensitized solar cells (DSSCs) utilizing both Pt and

CuMnS@rGO counter electrodes (CEs) were measured under simulated solar illumination with a light intensity of 100 mW cm⁻², as shown in (Fig 6). The photovoltaic performance

parameters for the CuMnS@rGO and Pt CEs, including short-circuit photocurrent density (J_{sc}), open-circuit photovoltage (V_{oc}), fill factor (FF), and power conversion efficiency (η), are listed in (Table 1). For the CuMnS@rGO CE, the DSSCs exhibited a J_{sc} of 19.859 mA/cm², a V_{oc} of 0.661 V, and a FF of 0.64, resulting in a power conversion efficiency (PCE) of 7.81%. Additionally, the long-term stability of DSSCs with Pt and CuMnS@rGO CEs was evaluated over 15 days, as illustrated in Figure 6b. The results showed negligible changes in the photoconversion efficiency values over this period, indicating that CuMnS@rGO is a highly stable and effective alternative CE material for DSSCs, comparable to the traditional Pt CE.

CONCLUSION

The results demonstrate the feasibility of using low-cost, earth-abundant transition metal ternary sulfides, such as CuMnS@rGO, as efficient and high-performance CE material in photovoltaic applications. The high catalytic activity of CuMnS@rGO for the regeneration of I₃⁻ species contributes to the observed photovoltaic energy conversion efficiency of 7.81%, which is comparable to that of traditional Pt CE (8.03%). This suggests that CuMnS@rGO holds great potential for commercialization and widespread adoption in DSSC technology, offering a more sustainable and cost-effective alternative to platinum-based CEs.

LITERATURE CITED

1. Brian O'Regan, Gratzel M. 1991. *Nature* 353: 737-740.
2. Iqbal, M.Z., Zakar, S., Haider, S.S., Afzal, A.M., Iqbal, M.J., Kamran, M.A. and Numan, A., (2020). Electrodeposited CuMnS and CoMnS electrodes for high-performance asymmetric supercapacitor devices. *Ceramics International*, 46(13), pp.21343-21350.
3. Indhumathy, M. and Prakasam, A., (2019). A one pot hydrothermal stimulated CdS-reduced graphene oxide (CdS/rGO) hybrid nanocomposite for high performance photovoltaic applications. *Journal of Materials Science: Materials in Electronics*, 30(16), pp.15444-15451.
4. Michael Raj, F. and Jeya Rajendran, A., (2017). Synthesis, structural, optical and dielectric properties of cadmium sulfide nanoparticles as photocathode for a solar cell. (pp. 159-170). Springer International Publishing.
5. F. Michael Raj and Jeya Rajendran, (2015) Synthesis and Characterization of Cadmium Sulfide Nanoparticles for the applications of Dye Sensitized Solar Cell", *International Journal of Innovative Research in Science, Engineering and Technology*, 4(1), pp. 56-60.
6. Alam, S.N., Sharma, N. and Kumar, L., (2017). Synthesis of graphene oxide (GO) by modified hummers method and its thermal reduction to obtain reduced graphene oxide (rGO). *Graphene*, 6(1), pp.1-18.
7. Michael Raj F., Jeya Rajendran A. (2017) In: Ebenezar J. (eds) Recent Trends in Materials Science and Applications. Springer Proceedings in Physics, vol 189. Springer, Cham.
8. Wang, P., Wang, J., Wang, X., Yu, H., Yu, J., Lei, M. and Wang, Y., (2013). One-step synthesis of easy-recycling TiO₂-rGO nanocomposite photocatalysts with enhanced photocatalytic activity. *Applied Catalysis B: Environmental*, 132, pp.452-459.
9. Raj, F.M., Rose, I.C., Sathish, R. and Rajendran, A.J., (2015) Synthesis and dielectric properties of CdO nanoparticles for the fabrication of dye sensitized solar cell. *Journal of Chemical and Pharmaceutical Sciences ISSN*, 974, p.2115.
10. Murali, S., Raj, F.M., Dhawa, S., Gopalkrishnan, N., Sathish, R. and Rajendran, (2016) A.J., Synthesis and characterization of graphene oxide as photoanode for dye sensitized solar cell. Ebenezar, J., (2017). *Recent trends in materials science and applications* (Vol. 189, p. 396). Springer.
11. Xue, J., Wu, L., Hu, N., Qiu, J., Chang, C., Atobe, S., Fukunaga, H., Watanabe, T., Liu, Y., Ning, H. and Li, J., (2012). Evaluation of piezoelectric property of reduced graphene oxide (rGO)-poly (vinylidene fluoride) nanocomposites. *Nanoscale*, 4(22), pp.7250-7255.
12. Raj, F.M. and Rajendran, A.J., (2015). Synthesis and characterization of cadmium sulfide nanoparticles for the applications of dye sensitized solar cell. *Volume 4, Special Issue 1*, pp 44-48.
13. Venkatesh, M.S. and Raghavan, G.S.V., (2005) An overview of dielectric properties measuring techniques. *Canadian biosystems engineering*, 47(7), pp.15-30.
14. Shamraiz, U., Hussain, R.A. and Badshah, A., (2016). Fabrication and applications of copper sulfide (CuS) nanostructures. *Journal of Solid State Chemistry*, 238, pp.25-40.
15. Saranya, M., Santhosh, C., Ramachandran, R., Vinoba, M., and Grace, A.N., (2014) Hydrothermal growth of CuS nanostructures and its photocatalytic properties. *Powder technology*, 252, pp.25-32.
16. Pujari, R.B., Lokhande, A.C., Yadav, A.A., Kim, J.H. and Lokhande, C.D., 2016. Synthesis of MnS microfibers for high performance flexible supercapacitors. *Materials & Design*, 108, pp.510-517.
17. Michaelraj F, Pandiyarajan O, Aruldoss M, Prabhu M, Dhawa S. 2023. Synthesis, characterization, biological activity of 1-Aryl-4-Phenylamino-1-Butanone Hydrochloride. *Research Journal of Agricultural Sciences* 14(4): 898-901.